Intelligent image analysis for image-guided laser hair removal and skin therapy

Brian Walker[1], Thomas Lu[2*], Tien-Hsin Chao[2]
[1]Mt. San Antonio College, Walnut, CA, [2]Jet Propulsion Laboratory/California Institute of Technology, Pasadena, California, 91109

ABSTRACT

We present the development of advanced automatic target recognition (ATR) algorithms for the hair follicles identification in digital skin images to accurately direct the laser beam to remove the hair. The ATR system first performs a wavelet filtering to enhance the contrast of the hair features in the image. The system then extracts the unique features of the targets and sends the features to an Adaboost based classifier for training and recognition operations. The ATR system automatically classifies the hair, moles, or other skin lesion and provides the accurate coordinates of the intended hair follicle locations. The coordinates can be used to guide a scanning laser to focus energy only on the hair follicles. The intended benefit would be to protect the skin from unwanted laser exposure and to provide more effective skin therapy.

Key Words: skin therapy, laser hair removal, image processing, hair follicle identification, laser scanning.

1. INTRODUCTION

Laser has been widely used in skin therapy such as hair removal and skin rejuvenation [1]. Current laser hair removal products apply laser or white light on an area of the skin indiscriminately. High energy laser may cause unintentional damage on the lesion, moles, or other part of the skin in the area if the intended purpose is only to remove the hair follicles. It is desired to locate the hair follicles so that we can focus the light to the locations. Various image processing and pattern recognition algorithms have been developed in the past 30 years for many computer vision applications [2]. We present a multi-stage Automated Target Recognition (ATR) system developed at JPL for the skin hair follicle detection application [3-7]. The ATR system involves three primary components: first, an optical correlation is used to find the regions of interests (ROI) that possibly contains a target; second, feature extraction is performed to convert a ROI from a small image into a feature vector; Lastly, a classifier, such as an adaptive boosting (Adaboost) decision tree [8] or neural network [9] is used to classify the feature as either containing the desired target or failing to contain the target.

* e-mail: Thomas.T.Lu@jpl.nasa.gov , Tel: (818) 354-9513

2. AUTOMATIC TARGET RECOGNITION ARCHITECTURE

2.1 Optical correlation using wavelets

Wavelets are commonly used in signal analysis and compression algorithms because of their ability to encode both spatial and frequency information [10]. The most common method for correlation of a data stream with a wavelet is to integrate the product of the incoming data stream and the wavelet which is to be correlated in the following manner:

$$W_{\Psi}(f(x))_{(a,b)} = \int_{-\infty}^{\infty} W(x,a,b)f(x)dx \quad (1)$$

Where W(x,a,b) is the particular variant of the mother wavelet with parameters 'a' and 'b', and f(x) is signal to be identified. The parameter 'a' serves to stretch the wavelet horizontally, and the parameter 'b' changes the center point of the wavelet. To understand how this process works, take for example the f(x) = sin(x) in Figure 1 (a), and W(x,a,b) = the negative of the second derivative of a Gaussian function, commonly called the Mexican hat wavelet in Figure 1 (b).

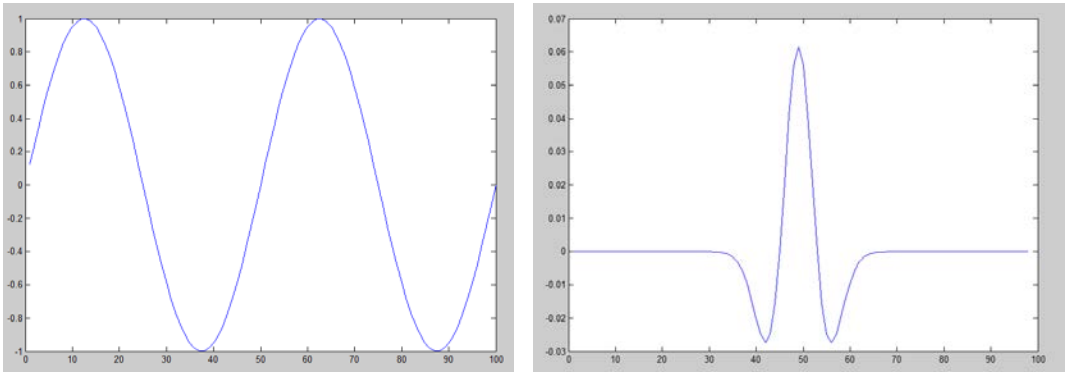

(a) (b)

Figure 1: Comparison of a sine wave and a Mexican hat wavelet: (a) a plot of sine function (b) a plot of the Mexican hat wavelet

Using a range of scaling factors from 1 to 20, we can see the correlation between the two functions in Figure 2, is created. The horizontal axis is the same axis as the original sine wave, and the vertical axis is the scaling factor of the wavelet. Dark areas in the graph represent weak correlation, and bright locations indicate strong positive or negative correlation. It is clear from this plot that a scaling factor of 13 results in very bright maximums for the central peak and valley of the sine function in Figure 1 (a). In this manner it is possible to determine both the scale, and location of a feature in a given signal. If the scale is known in advance, it is possible to accurately determine the location of a feature.

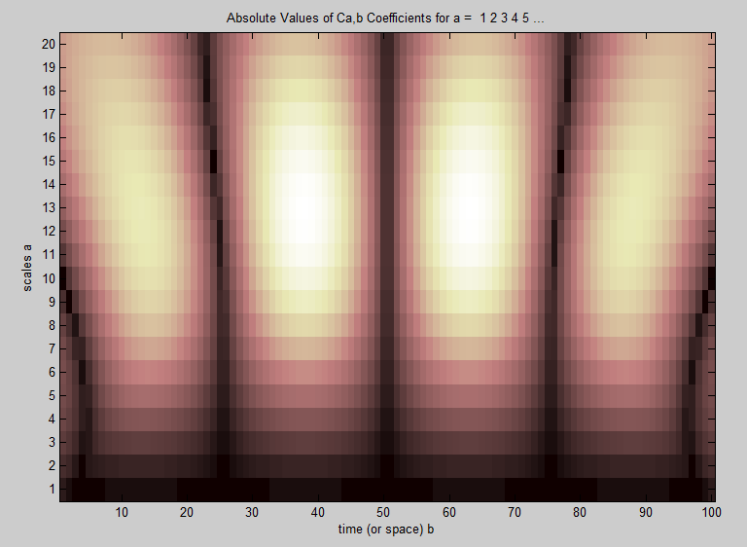

Figure 2 – the correlation plot corresponding to a continuous wavelet transform of a sine function. The plot includes scaling factors 1 to 20.

2.2 Feature Extraction

If a computationally intensive algorithm is run on a large data set, the processing time quickly becomes unreasonable for a real time device. This encourages the use of optical correlation, such as the wavelet transform to divide the image into regions of interest and non-interest. This quick analysis facilitates a more thorough investigation of the image. Once these interesting regions are chosen, a smaller subset of data can be extracted and processed further. Each element in this subset is known as a feature vector, and the selection of appropriate features to include in that vector is integral to successful classification.

A feature vector initially is constructed from a square of pixels centered on the region of interest found in the optical correlation stage. This square is in fact a small image cut from the original image, on which further mathematical analysis can be performed. Some common features include the standard deviation, mean, mode, skewness and kurtosis of pixel values. Additional features may include the entropy, properties obtained from morphological operations, information contained in the frequency domain, and many others.

2.3 Classification using Adaptive Boosting

Boosting is a machine learning algorithm which applies many weak learners together to create a strong learner. A weak learner is a discriminator which is able to successfully categorize targets and non-targets at least better than 50% of the time. Adaptive Boosting is a common algorithm using this premise, and its application can be understood from the following images.

As shown in Figure 3, consider a set of feature vectors consisting of a 2-tuple of Cartesian coordinates, the first image shows a dataset, which has been bisected by a weak learner. The majority of the white dots are on the lower side of the line, thus the learner has successfully separated some of the non-targets (gray dots) from the targets (white dots). The second image shows 5 weak learners operating on the same data set, it is clear that the majority of the targets are contained inside of the pentagon, and that the majority of the non-targets are outside the pentagon. This concept can be generalized to n-dimensional space, thus accommodating feature vectors of arbitrary dimension.

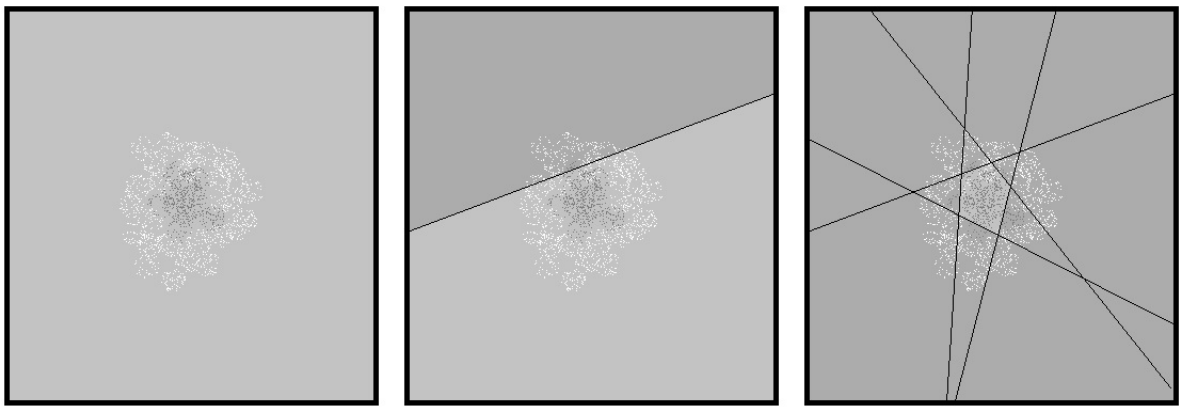

(a) *(b)* *(c)*

Figure 3 – Illustration of the adaboosting principle: (a) representation of two classes of objects in white and gray dots; (b) trying to segment white and gray dots using a linear fit (weak learner); (c) application of 5 linear fits successfully segments the data.

3. APPLICATION TO HAIR FOLLICLE IDENTIFICATION

3.1 Correlation of follicles with a Mexican hat wavelet

For the purposes of hair follicle identification, it is important to understand the nature of the image in numerical form. Take for example the following image in Fig. 4 (a).

[a] 

[b] 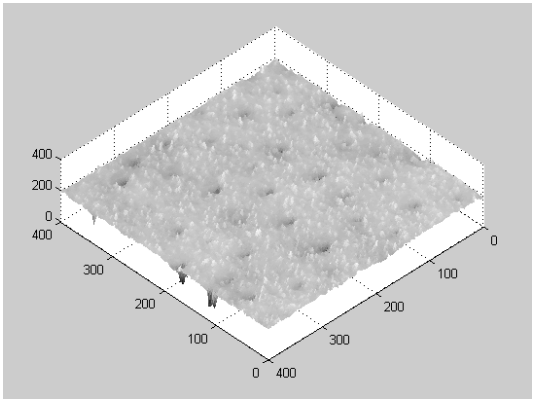

(a) **(b)**

Figure 4: An image of the hair follicles: (a) high resolution picture of human skin; (b) the same image as a surface plot.

Figure 4 (a) presents a number of hair follicles on which we can observe a trend. When this image is converted to grayscale, and then plotted as a surface in three dimensions, Figure 4 (b) is obtained. Immediately evident is that the regions from the original image that contain hair follicles are now local minima in the surface plot. This fact is even more evident when a single hair follicle is viewed in cross section in Figure 5 (a).

This trend very nearly resembles an inverted version of the second derivative of a Gaussian wavelet, commonly referred to as a Mexican hat wavelet, Figure 5 (b). Though there is some jaggedness to the edges of the real data, the wavelet transform should be able to correlate these two functions very nicely. When the input data, Figure 5 (a), is operated on using a continuous wavelet transform, the result is the following plot in Figure 6.

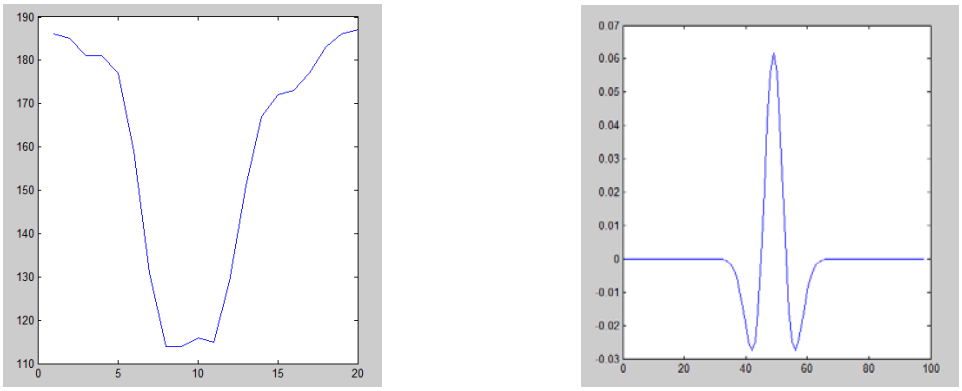

(a) (b)

Figure 5 : (a) a plot of the cross section of a hair follicle; (b) a plot of the Mexican hat wavelet.

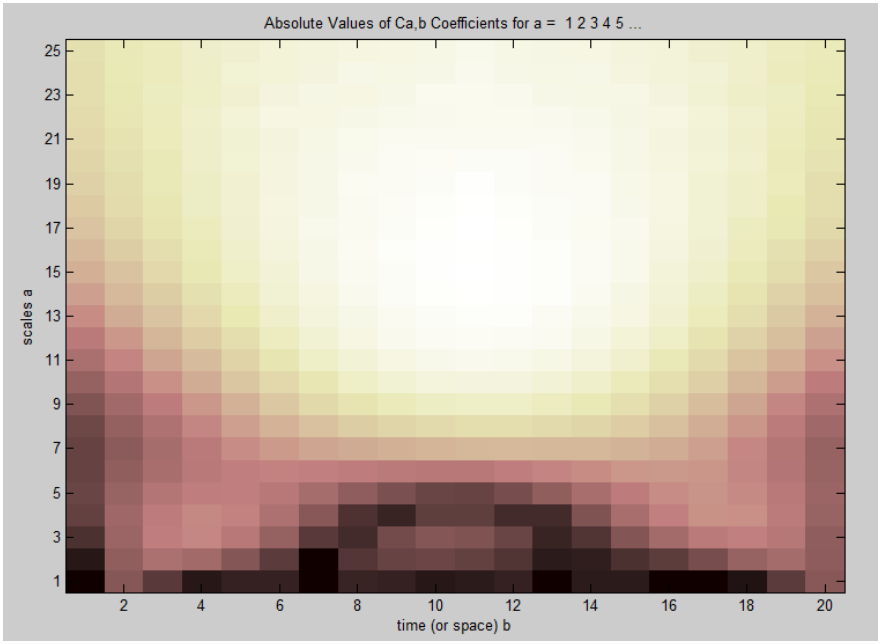

Figure 6: A plot of the correlation between the Mexican hat wavelet and the cross section of the hair follicle using scaling factors of 1-25.

It is apparent from Figure 6, that the hair follicle is most strongly correlated with a scaling factor of 15-17, so inclusion of those scales in the optical correlation phase will improve performance.

Figure 7 demonstrates how the output from the continuous wavelet transform can be used to isolate hair follicles in a grayscale image. Image [a] is the original test image in grayscale; image [b] is the correlation image that results from a continuous wavelet transform, using scales 15-17, of the image. Negative correlation peaks have been removed for clarity. Image [c] is the grayscale image [a] with a contour plot of image [b] superimposed. It is clear from image [c] that the continuous wavelet transform is capable of finding hair follicles in the image, with a tolerable level of error.

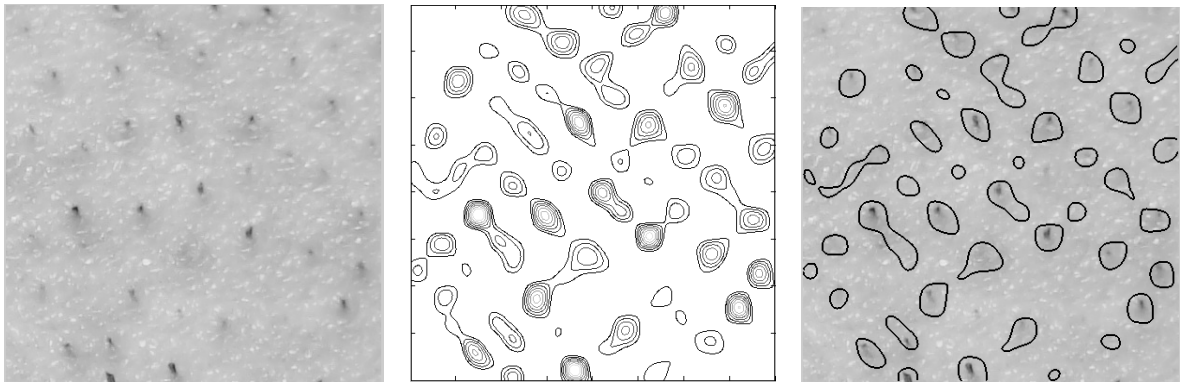

(a) (b) (c)

Figure 7: Experimental results of wavelet enhancement of hair follicle features. (a) the original skin image in grayscale; (b) the output from the wavelet optical correlation stage; (c) an overlay of a threshold and contour map of (b) onto (a).

3.2 Selection of appropriate features

The wavelet correlation gives regions of interest (ROIs) from the image. The next step is to extract features from the ROIs for hair follicles identification.

For this particular implementation of target recognition, the following feature vectors were chosen.

1. Entropy – A statistical measure of the randomness present in the region of interest.
2. Skewness – A statistical description of the distribution of pixel values present.
3. Mean – The average of the pixel values.
4. Standard Deviation – A measure of how widely distributed the pixel values are.
5. Feature Area – A morphological operation that describes how large of a region contains pixels which are more than two standard deviations below the mean.
6. Euler Number – A morphological operation which is equal to the number of individual elements in an image minus the number of holes in those elements.

7. Frequency Amplitude Ratio – An operation which compares the maximum positive height and negative height of the real part of the Fourier transform of the region.

8. Minimum Value – The lowest value pixel present in the feature.

9. Correlation Peak – The average of all of the pixels in the correlation plane associated with the feature.

10. Peak to Side Lobe Ratio – The ratio of the correlation peak to the average of the elements adjacent to the feature.

Figure 8 shows the typical regions of interest found in a skin image. The region in Figure 8 (a) does not contain a hair follicle, whereas the region in Figure 8 (b) does. This may be visible to the naked eye, but by using feature vectors it is now visible in the form of data. Figures 8 (c) and (d) contain the feature vectors associated with regions (a) and (b), and there are several notable differences. First, the magnitude of the entropy of region (b) is nearly double that of region (a). Second, the sign of the Skewness is opposite for each region. Third, the

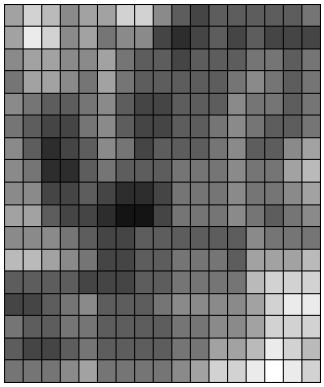

(a)

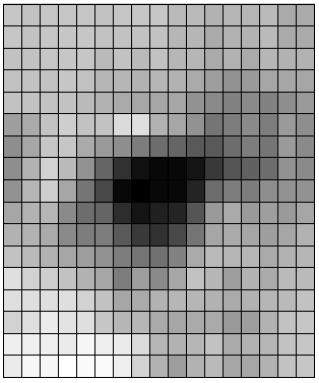

(b)

2.8940	Entropy	4.6123
0.7572	Skewness	-1.4499
170.2531	Mean	157.5617
2.0087	STD	8.1030
139.5000	F.A.	53.3750
8.0000	Euler	1.0000
0.8463	FAR	2.0791
165.0000	Min	128.0000
6.5451	Peak	27.8348
0.2339	PSR	0.5670

(c) (d)

Figure 8: Comparison of feature vectors in the ROIs: (a) a region of interest not containing a follicle; (b) a region of interest that does contain a follicle; (c) feature vector for the ROI in (a); (d) feature vector for the ROI in (b).

standard deviation for region (b) is more than 4 times as large as (a). Fourth, the feature area is much smaller in region (b). Fifth, the Euler number is unity for the region (b), and much larger for region (a). Finally, the correlation peak for region (b) is much higher than the correlation peak for region (a).

These 6 major differences in feature vectors allows for successful differentiation between the two images. Other images have different values for their feature vectors, and those features which did not vary significantly in these images may play a more significant role in other images.

3.3 Adaboost classification

In the multi-stage ATR system, we intentionally set the threshold low in the first stage optical correlation operation in order not to miss any true target. The output from the optical correlation stage inherently contains many false positives. These false positives can be reduced significantly through the application of adaptive boosting in the later stage of the ATR process.

Figures 9 shows the processing of the image from its raw state, (a), the output from the first-stage wavelet optical correlation, (b), and the results after the last-stage adaptive boosting is applied, (c). The gray boxes indicate the false positives; and the black boxes are confirmed target locations identified by the processor. Comparing Figures 9 (b) and (c), we can see that many false positives are eliminated by the adaboost process. It is important to note that the final image is not completely free from false positives. In Figure 9 (c), it contains 16 false positives, 10 of which are overlapping true positives and can be removed with further processing, 2 of which are due to the ground truths not containing follicles at the borders of the image, which leaves 4 false positives un-accounted for. These may in fact be hair follicles that are not apparent to the naked eye, and as the truth checking is based on human observation, they would not be found in the ground truths list.

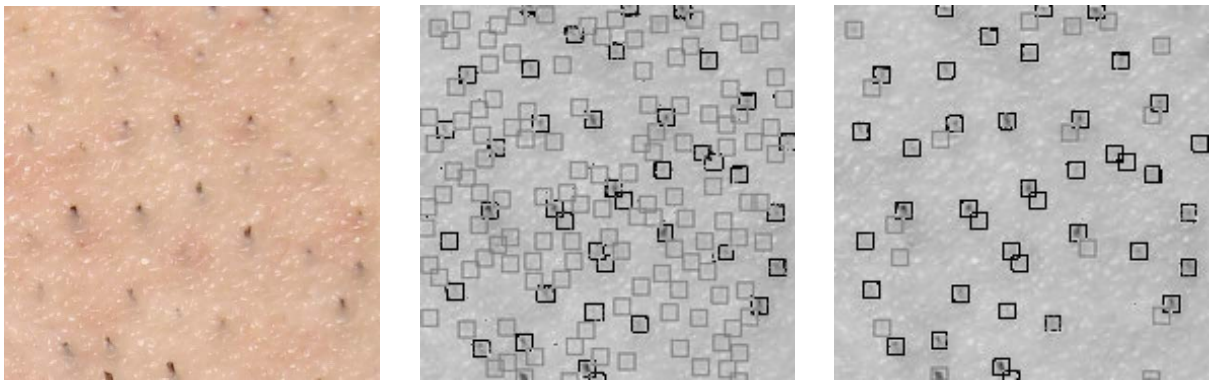

(a) (b) (c)

Figure 9: Identification of the hair follicles by a three-stage ATR system: (a) the original skin image; (b) an image of the skin with squares indicating regions of interest from the first-stage optical correlation, gray boxes indicate false positives, and black indicates true positives; [c] the output after the third-stage adaptive boosting is applied.

When the same process is applied to skin that is exposed to a higher level of ambient lighting, the following images are produced in Figure 10. We can see the results from Figure 10 (c) have less false positives. It is clear that lighting conditions play a significant role in eliminating the duplication of true positives found in the first image, but it is also apparent that there may be some hair follicles that are not being found. This is a preferable situation to the one where all of the follicles are found, because as was mentioned earlier, the lasing of a false positive could result in unnecessary tissue damage.

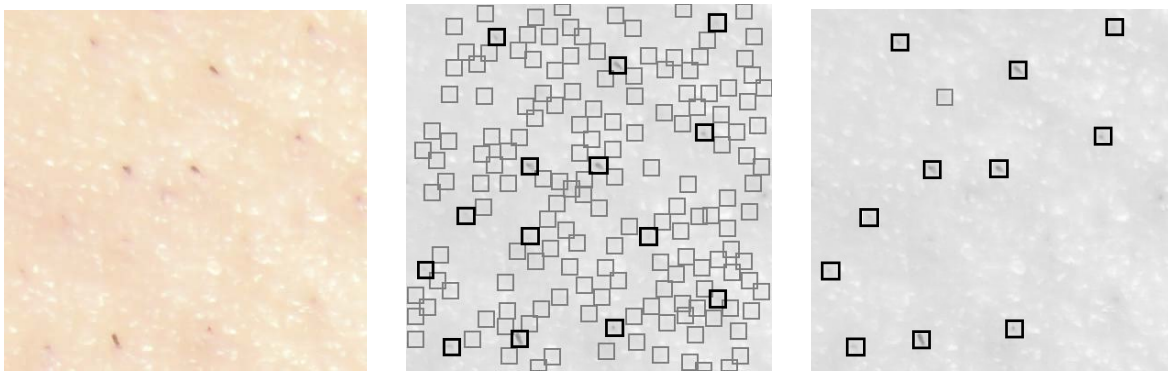

(a) (b) (c)

Figure 10: ATR results in a brightly lit image: (a) original skin image; (b) output from the first-stage correlation stage; (c) the output after the third-stage adaptive boosting is applied.

4. EXPERIMENTAL RESULTS AND DISCUSSIONS

In the experimental testing, skin images were cut into smaller sizes. Each image is 400x400 pixels, and the computer has a 3.16 GHz processor and 4 GB of ram. The output from the ATR system has the best performance on brightly lit sections of skin, with freshly shaven hair.

Based on the outputs from the three-stage target recognition program, the following free response receiver operating characteristic, or FROC, curves were generated. The first FROC curve, in Figure 11, is operating on a data

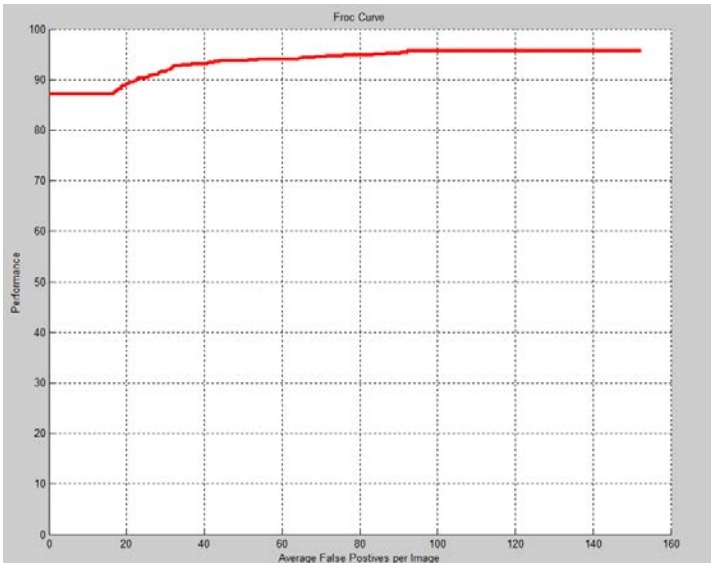

Figure 11: Free response receiver operating characteristic *(FROC) curve for variable lighting conditions: Y-axis: performance – percentage of true identification of hair follicles; X-axis: average number of false identification per image.*

set with varying lighting conditions, but has excellent performance in the 0-5 false positives per image region. It does not approach 100 percent accuracy, even as the false positives per image approach 300, but this is not a concern as current state of the art laser hair removal procedures require several treatments, and a real time system would have many more opportunities to find follicles which avoid initial classification. Under these conditions, a lower bound for the performance is 77 percent identification with a maximum of 2 false positives per image.

For the purposes of hair removal, minimization of false positives take precedence over the pursuit of 100 percent accuracy, as the consequences for leaving a hair behind are much less significant than those associated with lasing a non-hair follicle region. Additionally, follicles that are not identified in the first image may be more apparent when viewed from a different angle. Accordingly, if this system were to be applied to a real time data stream, there would be several opportunities to identify follicles that escape initial identification.

The skin and hair have various colors. The contrast between the hair and the skin would affect the performance of the ATR system. Proper lighting would help the detection of the hair follicles in the skin images. The RGB color channels have been exploited to find the maximum contrast of the image. Hair follicles may be under the skin that may be hard to see from above the skin. Near IR light in the 700nm – 1200nm may penetrate the skin and reveal the hair follicle under the skin. The CCD and CMOS cameras are sensitive to the NIR light. If the ATR system were to include a NIR lighting, the ATR system may exhibit improved false positive rejection, and the ability to see a few millimeters beneath the epidermis. This would allow for greater precision during the lasing process.

5. CONCLUSIONS

It is evident that a properly tuned ATR system can identify hair follicles with a great degree of accuracy, or with a sufficient degree of accuracy and a large safety margin. Our preliminary experiments with a multi-stage ATR system have shown accurate identification of hair follicles in the skin images. Under conditions that are likely to be present in a medical procedure, specifically the presence of sufficient lighting, and the recent shaving of the test area, the autonomous target identification system could be safely used in conjunction with a laser scanning system to autonomously lase hair follicles. The precision benefits of using an autonomous system would allow for a smaller focal point, thus causing less damage to surrounding tissue.

ACKNOWLEDGEMENTS

This research was carried out at the Jet Propulsion Laboratory, California Institute of Technology under a contract with the National Aeronautics and Space Administration and was sponsored by the SIRI internship program through NASA, JPL, and Caltech.

REFERENCES

1. http://www.skincareguide.ca/treatments/laser_hair_removal.html.
2. Nalwa, V. S., “A guided tour of computer vision,” Addison-Wesley (1993).
3. T. Lu, C. Hughlett, H. Zhou, T-H. Chao, and J. Hanan, “Neural network post-processing of grayscale optical correlator,” *SPIE Proceedings,* **5908** (2005).

4. W.N. Greene, Y. Zhang, T. Lu, and T-H. Chao, "Feature extraction and selection strategies for automated target recognition," *SPIE Conference* **7703** (2010).
5. O. Johnson, W. Edens, T. Lu, and T-H. Chao, "Optimization of OT-MACH filter generation for target recognition," *SPIE Conference* **7340** (2009).
6. T. H. Lin, T. Lu, H. Braun, W. Edens, Y. Zhang, T-H. Chao, C. Assad, and T. Huntsberger, "Optimization of a multi-stage ATR system for small target identification," *SPIE Conference* **7696** (2010).
7. H. Zhou, C. Hughlett, J. Hanan, T. Lu, and T-H. Chao, "Development of streamlined OT-MACH-based ATR algorithm for grayscale optical correlator," *SPIE Optical Pattern Recognition XVI* **5816**, 78–83 (2005).
8. Schapire,R.E., Singer,Y., " Improved boosting algorithms using confidence-rated predictions," Machine Learning 37(3), 297-336 (1999).
9. Jain, A., J. Mao, and K.M. Mohiuddin, "Artificial neural networks: A tutorial," *IEEE Computer* **29**, 31–44 (1996).
10. Chui, C. K. "An Introduction to Wavelets," Academic Press (1992).